JOURNAL OF MATERIALS SCIENCE **39** (2004) 771–778

Electrophoretic deposition of monochrome and color phosphor screens for information displays

J. B. TALBOT*
Chemical Engineering Program, University of California, San Diego, 9500 Gilman Drive, La Jolla, CA 92093-0411, USA
E-mail: jtalbot@ucsd.edu

E. SLUZKY
7739 Ivanhoe Ave., La Jolla, CA 92037, USA

S. K. KURINEC
Microelectronic Engineering, Rochester Institute of Technology, Rochester, NY 14623-5604, USA
E-mail: skkemc@rit.edu

This paper reviews our research on the electrophoretic deposition (EPD) of phosphors for the processing of monochromatic and color screens for information displays. Our investigation began with the study of the fundamentals of the EPD process for phosphors. The processing variables which enhance the adhesion strength of phosphor deposits were determined. The optical performance of phosphors deposited by EPD was shown to be not affected by the process itself nor by the conditions which enhance phosphor adhesion. Processes developed to produce high-resolution color screens by combining EPD and photolithography techniques are described. Also, a method to electrophoretically deposit phosphor in a thermo-reversible gel from mixtures of poly(butyl methacrylate) and isopropanol was examined.

1. Introduction

All phosphor screens must meet a number of requirements for use in an information display [1]. The deposit thickness must be optimized to ensure pin-hole free coverage, yet not reduce light emission due to internal absorption. The packing density should be optimized for the best light output at specific excitation conditions. The screen must be uniform to ensure consistent optical performance. The amount of non-luminescent material needs to be minimized. Finally, the deposit must have sufficient adhesion strength to withstand handling during manufacturing, as well as during use.

Electrophoretic deposition (EPD) of powder phosphors, typically 0.5–10 μm diameter, is used in the manufacturing of displays, particularly high-resolution screens [2]. During EPD, charged phosphor particles suspended in a liquid are deposited onto a conductive substrate under the influence of an electric field. Grosso *et al*. [3] reported the deposition of luminescent materials from isopropyl alcohol (IPA) and the effect of water in the bath on the deposition. Sluzky and Hesse [4] studied the EPD of phosphor screens and concluded that the screen can demonstrate brightness equal to coatings made by standard settling methods and are capable of very high resolution. Our group has systematically investigated the fundamentals of EPD process for phosphors, including the dissociation of nitrate salts in IPA [5, 6], the zeta potential of charged phosphor particles [5, 7], as well as the formation of the adhesive agents [6, 8]. The deposition rates of the phosphor and binder were modeled [9, 10]. The factors which affect the adhesion strength of the deposited phosphors were identified [11, 12]. The optical performance of phosphor screens was tested and was found not to be affected by the process itself nor by the conditions which enhance phosphor adhesion under 1–4 kV excitation voltage applicable to field emission displays (FEDs) [13]. Three new screening methods were developed: two for color displays by combining EPD and photolithography [14, 15] and another by EPD in a thermoreversible gel [16]. Our research results will be reviewed here; descriptions of the experimental apparatus and procedures with details of the results can be found in the references.

2. Fundamentals of the EPD process

To understand EPD, the process was divided into the following fundamental steps: (a) the charging of the particles in suspension, (b) the transport of the particles under the influence of an electric field, and (c) the deposition and adherence of the particles onto a substrate. The electrophoretic deposition bath of

*Author to whom all correspondence should be addressed.

TABLE I Limiting conductivities (Λ_o) and dissociation constants (K_D) of nitrate salts in IPA

Reaction	Λ_o(cm^2/mole-ohm)	K_D (M)
$NaNO_3 \rightarrow Na^+ + NO_3^-$	17	3×10^{-4}
$Mg(NO_3)_2 \rightarrow Mg(NO_3)^+ + NO_3^-$	18	6×10^{-5}
$Mg(NO_3)^+ \rightarrow Mg^{2+} + NO_3^-$	120	2×10^{-7}

interest in our studies is a suspension of phosphor particles in isopropyl alcohol (IPA) (4 g/l) which contains dissolved nitrate salts (typically 10^{-3} M $Mg(NO_3)_2$) and small amounts of water ($\sim$1 vol%). The nitrate salt dissociates slightly, providing ions to charge the particles positively. Therefore, the approach taken was to (a) investigate the dissociation behavior of nitrate salts in IPA, (b) study the effects of phosphor chemistry and suspension medium on the zeta potential of the particles, and (c) study the effects of the EPD process conditions and model the deposition rates.

The conductivity of various nitrate salts in IPA was measured and analyzed using the Ostwald dilution law to determine the conductivity at infinite dilution and dissociation constants as shown in Table I [5]. The mobility of the ions can be determined with the use of the limiting conductivity and concentration of ions can be calculated from the dissociation constant [5, 10]. The dissociation constants are very low and in the concentration range of 10^{-4} to 10^{-3} M $Mg(NO_3)_2$ typically used in EPD baths, $MgNO_3^+$ is the predominant cation available to charge the phosphor and to form the binder.

The zeta potentials of several oxide, sulfide, and oxysulfide phosphors were measured in IPA and in IPA containing nitrate salts and water [7]. The zeta potentials of phosphors in pure IPA were negative. With the addition of 5×10^{-4} M nitrate salt, the zeta potentials of nearly all the phosphors became positive. A more focused study measured the zeta potentials of Zn_2SiO_4:Mn (P-1) and ZnS:Ag (P-11) phosphor particles in IPA under a wide range of nitrate salt concentrations and pH values [5]. The zeta potential was negative (~ -50 mV) at salt concentrations less than 10^{-6} M. As the salt concentration increased, the zeta potential increased and became positive, reaching a maximum ($\sim$50 mV) at 10^{-5} M. In IPA or IPA with 10^{-5} M magnesium nitrate, the zeta potential was positive at pH < 6, but became negative for pH > 6. At higher salt concentrations of 10^{-4} and 10^{-3} M, the zeta potential remained positive for all pH values. Therefore, the zeta potential is dependent upon the nitrate salt concentration and pH.

During EPD, electrolysis of the water present in the IPA creates a basic environment at the cathode. Thus, $MgNO_3^+$ reacts with the hydroxide ions to produce magnesium hydroxide [7, 8], as follows:

$$2H_2O + 2e^- = H_2(g) + 2OH^-$$

$$MgNO_3^+ + 2OH^- = Mg(OH)_2 + NO_3^-$$

By carefully controlling the amount of water in the IPA bath, it was determined that alkoxide formation can also occur, which can contribute to the binder formation [12]:

$$Mg^{2+} + 2C_3H_7OH = Mg(C_3H_7O)_2 + 2H^+$$

$$Mg(C_3H_7O)_2 + 2H_2O = Mg(OH)_2 + 2C_3H_7OH.$$

When the water concentration in the EPD bath is low (<1vol%), alkoxide predominately forms, whereas at high water content (>5 vol%), all of the alkoxide is converted to the hydroxide. At intermediate water concentrations, the binder is a mixture of the two materials. Thus, the role of the magnesium nitrate in the EPD bath is to charge the phosphor particle positively, to maintain the positive zeta potential at high pH at the cathode, and to form the adhesive material.

The amounts of deposited phosphor and magnesium hydroxide binder were simply modeled by integrating the flux of material over time multiplied by the fraction of material adhering [9, 10]:

$$M = \int_0^t \alpha C v A \, dt$$

where M is the mass of material deposited (mg) in time $t(s)$, α is the fraction of material reaching the cathode which adheres, C is the concentration of the material (phosphor or $MgNO_3^+$) in suspension (mg/cm^3), v is the velocity under the influence of the electric field (cm/s), and A is the area of the cathode (cm^2). The velocity is due only to electrical migration and is the product of the mobility (u) and the electric field strength (E), which can be calculated from the average current density (i) during deposition by $v = uE = u(i/kA)$, where k is the specific conductivity of the solution. For the phosphor particles, the mobility was determined from the measured zeta potential (ζ) using the Smoluchowski equation, $u = \zeta\varepsilon/\mu$, where ε is the permittivity (18.3) and μ is the viscosity (2 cP) of IPA. The mobility of $Mg(NO_3)^+$ was calculated from $u = \Lambda_o t_+/F$, where t_+ is the cation transference number ($\sim$0.4) and F is Faraday's constant. The concentration of $Mg(NO_3)^+$ was multiplied by the molecular weight of $Mg(OH)_2$, as this is the species that deposits. With conductivity measurements of $Mg(NO_3)_2$ in IPA, the specific conductivity, the limiting conductivity, and the concentration of $Mg(NO_3)^+$ were determined [5]. The deposition rates of both the phosphor and magnesium hydroxide predicted from this simple model agreed with experimental results provided that the $Mg(NO_3)_2$concentration was greater than $\sim 10^{-4}$ M [10]. This minimum concentration maintains a positive zeta potential near the cathode and provides the necessary amount of binder to adhere the particles (α equal to 1).

3. Adhesion of EPD deposits

Adequate adhesion of the phosphor on the screen is important as the phosphor coating must endure several processing steps before final display assembly, and during use the display must tolerate shocks and vibrations. As discussed, hydroxides and alkoxides formed via cathodic precipitation are the binder materials for the phosphor particles in the deposited layer [6, 8] with a minimum amount of binder necessary

for particle adhesion [10]. A limitation of phosphor screens made by EPD is the low adhesion strength of the deposit. Therefore, the effects of the inherent EPD processing conditions on the adhesion strength and ways to enhance adhesion of deposited phosphors were investigated [12].

The adhesion strength of a deposit was tested by removal of particles by applying a jet of nitrogen gas perpendicular to the coating [17]. The adhesion strength was determined by one of two methods. The first method is qualitative for the weak deposits, using the weight% of particles remaining on the substrate after testing as the adhesion strength. The second method provides a quantitative measurement for the strong deposits by relating the width of the ring of material removed from the substrate to the shear stress on the substrate, which equals the adhesion strength (in the range of 0.08 to 0.4 N) [17].

The variables investigated were phosphor concentration, type of phosphor, particle size distribution, water content in the bath, salt concentration and the type of salt (e.g., $Mg(NO_3)_2$, $Y(NO_3)_3$ and $La(NO_3)_3$) in the bath, and chemical additives (e.g., cellulose and glycerin). Unless otherwise stated, all depositions were made from an IPA bath with 10^{-3} M $Mg(NO_3)_2$ with a ZnS:Ag phosphor particle loading of 4 g/l. Samples were baked at 425°C for 1 h after deposition; deposit densities were 2 mg/cm^2. After baking the binder is completely converted to MgO [9]. Table II lists those parameters which had no effect on the adhesion strength of EPD phosphor deposits and these have been discussed elsewhere [11]. The location of the binder was determined to be the interstitial region between the particles. Thus, the adhesion strength of the EPD phosphor deposits is due solely to the contact points between the particles. Additional binder material, which may fill the interstitial region or cover the deposit, does not enhance the adhesion strength. Table III lists those variables, in order of decreasing importance, which did affect the adhesion strength of phosphor deposits. The results as listed in Table III will be summarized, but the adhesion data are presented elsewhere [11, 12].

Glycerin, which is commonly used industrially to disperse particles, had the largest effect on the adhesion strength. Virtually no particles were dislodged by the adhesion test on the deposits with 2 vol% added glycerin to the bath. This increase in adhesion strength is likely due to dispersion of smaller particles and polymerization of the glycerin upon baking. Added water, up to 5 vol%, to the deposition bath greatly enhances the adhesion strength of EPD phosphor deposits. This increase in adhesion is due to the preferential deposition of $Mg(OH)_2$ instead of $Mg(C_3H_7O)_2$ as the binder with increasing water concentration in the bath. With water concentrations higher than 5%, the deposits became irregular and of poor quality due to excessive H_2 gas evolution at the cathode, which disrupts particle deposition. Since industrial systems typically do not control absorption of atmospheric moisture into the deposition bath or onto the deposit, there will always be high concentrations of water. While water content should be monitored, since excessive water can lead to irregular deposits, adsorbed water onto the deposit will increase the adhesion strength during handling prior to mounting and evacuation in a display device.

Post-deposition baking at 425°C for 1 h converts the $Mg(OH)_2$ and alkoxide binder to MgO. The MgO has a higher bond strength than the $Mg(OH)_2$ by 60%. The amount of MgO increased from 0.39 to 1.34 wt% in samples deposited from baths with 10^{-3} M and 5×10^{-3} M $Mg(NO_3)_2$, respectively. The particle size distribution also can effect the adhesion strength of phosphor deposits. It was found that a mixture of 20% 6 μm and 80% 3 μm mean diameter particles enhanced the adhesion strength, as well as increased the packing density. The change in porosity and packing of the deposit allows for more contact points for each particle. With more contact points, there are more adhesive points, leading to increased adhesion strength.

Three different salts, $Mg(NO_3)_2$, $La(NO_3)_3$ and $Y(NO_3)_3$, which are all commonly used in EPD processes (4), and combinations thereof, were studied. Using $Y(NO_3)_3$ in the deposition bath instead of $Mg(NO_3)_2$ was found to increase the adhesion strength. While the initial deposits from a $Y(NO_3)_3$ bath were weaker than those from a $Mg(NO_3)_2$ bath, the adhesion strength increased significantly after priming of the bath. The deposition bath is "primed" by depositing an initial sample, which usually has lower density than predicted by about 20% [17].

The type of phosphor used or the surface treatment of the phosphor particles can increase or decrease adhesion. For the P-11/$Mg(NO_3)_2$/IPA system, the salt concentration in the bath was optimized to control the zeta potential of the particle and the amount of binder. For the same deposition conditions, changing the phosphor material radically changed the adhesion strength of the deposit. Adhesion strengths for ZnS:Ag (P-11, 3 μm) and Zn_2SiO_4:Mn (P-1, 2.7 μm) deposits were approximately twice that of Gd_2O_2S:Tb (P-43, 2.3 μm).

TABLE II Parameters which did not affect adhesion strength of phosphor deposits

Parameter	Range
Applied voltage	50–800 V
Substrate coating	Al, Indium tin oxide
Deposit thickness	>1 mg/cm^2, < 7.4 mg/cm^2
Water soaking	1, 2, 3 min
MgO overcoating	0.5–2 mg
Phosphor concentration	0.5–8 g/l

TABLE III Parameters affecting adhesion strength of phosphor deposits

Parameter	Range	Effect on adhesion
Glycerin	1–2 vol%	Very large increase
Water	0–5 vol%	Large increase
Baking	425°C, 1 h	Increase
Particle size distribution	0–100%, 3 and 6 μm dia.	Increase
Salt identity	$Mg(NO_3)_2$, $La(NO_3)_3$, $Y(NO_3)_3$	Increase
Phosphor identity	P-11, P-1, P-43	Increase/decrease
Added cellulose	1–3.3 wt%	Decrease

This difference in adhesion strength most likely can be attributed to the different particle size distributions of these materials. High adhesion strength can be achieved most likely for any particle material, provided that the deposition conditions are optimized.

While cellulose is a useful additive for anodic EPD [18], it was found unsuitable for cathodic EPD of phosphor as it decreased adhesion. Also, the morphology of the deposits was rougher.

4. Optical performance of phosphor deposited by EPD

For the ultimate use in information displays, the optical performance of the phosphor screens produced by EPD must be tested [1, 2]. Therefore, the effects of the EPD processing conditions on the film thickness, packing density, and optical performance of phosphor deposits were investigated [12, 13]. The optical performance was evaluated by measurement of chromaticity and cathodoluminescent (CL) efficiency at low voltages (1–4 kV) applicable for field emission displays as well as high voltages (13–20 kV) in CRTs [4]. Of particular interest were the EPD processing conditions, which were found to enhance adhesion in Table III.

The packing density of deposits made at different applied voltages and with different deposit densities from 1 to 9 mg/cm^2 (5 to 40 μm thick) was constant at very high value of $\sim$55%. This suggests that the deposits with different thicknesses are homogeneous with a similar packing structure. Due to their similar structure, all of the deposits with different thicknesses made at 200 V demonstrated a similar CL reflection efficiency for deposit densities greater than 1 mg/cm^2. However, from transmission efficiency, an optimal thickness was found to be about 7 μm; this thickness corresponds to a deposit of about two layers of phosphor particles.

The EPD process does not affect the intrinsic efficiency or chromaticity of the phosphor [12, 13]. The introduction of glycerin or water into EPD baths, which dramatically increases the deposit adhesion strength, does not show any deleterious effect on the optical performance. Also, other conditions shown to enhance phosphor adhesion, such as the use of lanthanum nitrate in the bath or the particle size distribution, do not affect the optical performance of the phosphor deposit.

5. EPD processes for color displays

The development of new techniques for fabricating high-resolution, full-color screens is of interest, particularly for flat panel displays. Several techniques to pattern phosphor screens using EPD into triads of stripes have been developed in the 1970s [19–22]. However, inherent problems, such as large resistance drops and poor phosphor adhesion, associated with each of these processes has made them unacceptable as a viable alternative to conventional phosphor screening techniques [2]. Color vacuum fluorescent displays (VFDs) have been produced using EPD by selecting a conductive line for each color phosphor. Recently, ultra-high resolution color VFD screens for microdisplays on silicon chips were deposited with tricolor pixels as small as about 25 by 18 μm [23]. By combining a photolithographic technique similar to that developed by Mooney[24] and EPD, our phosphor screening processes were developed to deposit triads of phosphor stripes onto an indium-tin-oxide (ITO)-covered glass substrate with a line resolution of 100 triads of 75 μm stripes per inch [14, 15].

For the first method, the photoresist used was a mixture of 4.5 wt% polyvinyl alcohol (PVA), 0.45 vol% ammonia dichromate and a balance of distilled water [15]. The PVA solution was spin cast upon an ITO-covered glass substrate to a film thickness of $\sim$6 μm. Then the PVA was patterned using a mask aligner and a shadow mask to yield alternating 175 μm stripes of cross-linked PVA and 75 μm uncross-linked PVA stripes. The coating was then sprayed with warm water spray to dissolve and remove any uncross-linked PVA from the substrate. Next, the PVA-covered substrate was heated for several minutes to dry excess water and to complete the cross-linking reaction.

Small particle size (1–3 μm) green $ZnSiO_4$:Mn (P-1), red Y_2O_3:Eu (P-56), and blue ZnS:Ag,Cl (P-11) phosphors were deposited onto the 75 μm conductive striped regions of the substrate using EPD [15]. Successive depositions of the phosphors were performed by repeating the aforementioned steps. The shadow mask had to be aligned in precise registry with the edge of the previously coated stripes during each of the successive lithography steps. Also, the concentration of the ingredients within the solution bath was optimized according to the specific phosphor that was deposited [15].

The duration of exposure of the PVA-dichromate film to UV light was optimized in order to fabricate PVA stripes with a high degree of uniformity, edge straightness, water insolubility, and adhesion. The EPD conditions were optimized in order to comply with several requirements. A screen thickness of 4 to 6 μm was desired in order to maximize phosphor efficiency and resolution, while minimizing phosphor cross-contamination. Also, ample phosphor particle adhesion was required. The optimum deposition time and applied voltage for each phosphor were determined based upon the stripe thickness, continuity, edge resolution, and particle packing density. The phosphors were deposited in sequential order of P-1, P-56, and P-11 with deposition times of 20, 35, and 33 s, respectively. Also, little cross-contamination of phosphors was observed. It must be noted that higher line resolutions may be attainable with this method. The line resolution was constrained only by the shadow mask which had a resolution of 100 triads of lines per inch.

5.1. The trilayer process

In this process [14, 24], a cross-linked thick photoresist (AZ P4620, baked at 250°C) was employed to act as a mask. It was spun coated over the conducting seed layer to a thickness of $\sim$10 μm. The second layer of the trilayer scheme was an inorganic spin-on glass (SOG) (Accuspin 311) that acted as an etch stop in subsequent processing. For patterning, a thin ($\sim$1 μm) imaging positive resist was applied and exposed with the desired pattern.

Following the imaging resist development, SOG was etched in regions where phosphor deposition was required. To make the process efficient and manufacturable, dry etching was chosen. Reactive ion etching of SOG was carried out using a CF_4/H_2 plasma chemistry such that a reasonable selectivity was achieved between the resist and SOG. After etching SOG, the plasma chemistry was switched to oxygen to etch the hard-baked thick resist. The etching stopped on the conducting aluminum layer. The plasma residue was cleaned using a buffered HF-glycerin solution before carrying out the EPD of phosphor. The process described previously [14, 24] has been further improved by the development of a single chamber plasma process.

The commercial phosphors ($ZnSiO_4$:Mn, ZnS:Ag, and Y_2O_3:Eu) utilized had particle sizes varying from 2–6 μm. A timed deposition was performed to fill the trench, as shown in Fig. 1. The process was repeated for the other two color phosphors as depicted in the process flow diagram given in Fig. 2. Fig. 3 shows micrographs of finished screens: (a) with a triad pitch of 150 μm on a silicon substrate and (b) with a triad pitch of 50 μm on a quartz substrate. The red, green and blue (RGB) lines are separated by a black material ($MnCO_3$) also deposited by EPD. After EPD of the three phosphor lines, the process for black lines in between becomes self-aligned. The exposure tool utilized for this work was a 5× reduction standard wafer stepper commonly employed in semiconductor technology. The advantage is that the mask is not in contact with the screen and higher lithography resolution is easily attainable. However, the resolution is limited by the phosphor particle size. This can be observed in Fig. 3c, as a relatively smaller particle size for black material accounts for well-defined black lines in the screens.

5.2. EPD in a thermoversible gel

Another novel technique for depositing and patterning phosphors developed is EPD in a thermoreversible gel at specific points on the substrate [16]. A thermoreversible gel will melt upon heating and will resolidify when cooled. Thus, phosphors suspended in the gel matrix migrate in an applied electric field only when spot melting of the gel allows the phosphors to deposit on the substrate at that point. The melting and gelling may be repeated numerous times due to the physical bonds, unlike gels that are formed by chemical bonds which do not gel again once melted. The process as shown in Fig. 4 is described as follows.

Initially, a heated (liquid) solution of the polymer-solvent-phosphor system is coated on top of the substrate (e.g., ITO-coated glass). After the system is solidified (cooled), voltage is applied, creating an electric field. Spot-melting of the gel (e.g., by laser radiation) allows selective EPD of the phosphor to occur only at the desired spot or pattern. The electric field is removed and the gel is removed by melting, leaving only the deposited phosphor. This process may be repeated to deposit patterned multicolor screens. A possible advantage of utilizing EPD in a thermoreversible gel over the current methods which use organic photosensitive resins as lithographic structures [2] is its relative simplicity and avoiding the introduction of chromium (which decreases the phosphor brightness) and other chemicals (which may outgas and decrease the cathode performance) into the system.

First, an appropriate polymer-solvent system was required. Of the many polymer-solvent systems available [27], only a few solvents are suitable for EPD [28]. The system investigated was poly(butyl methacrylate) (PBMA), which forms a thermoreversible gel with

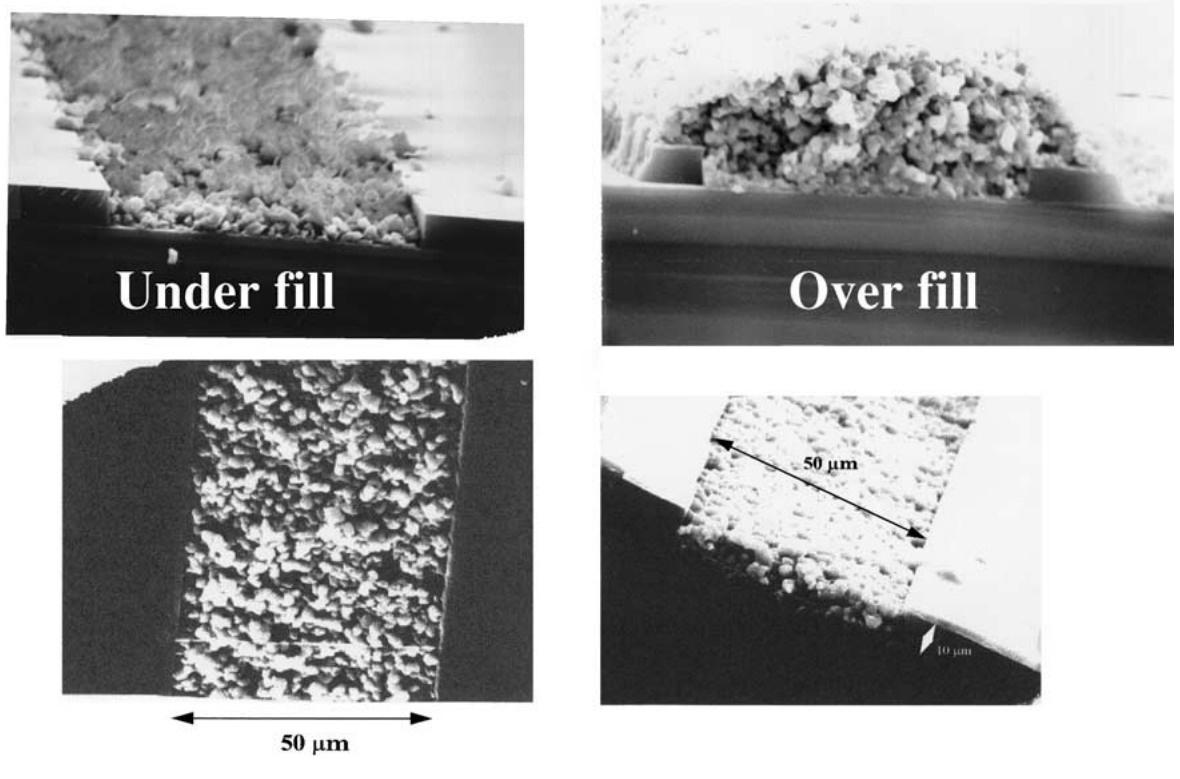

Figure 1 Cross-sectional scanning electron micrograph of a hardened resist trench filled with P-1 phosphor particles.

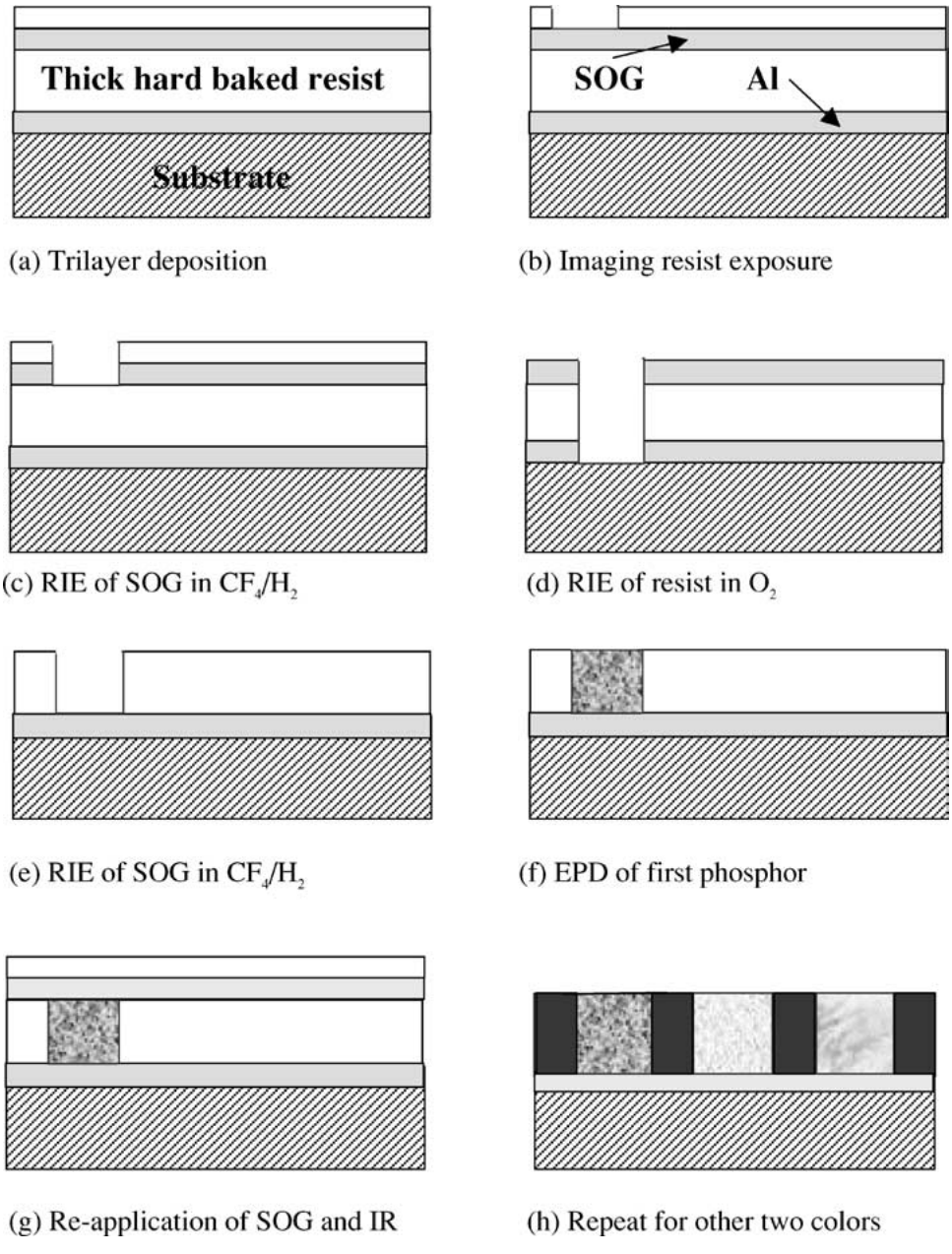

Figure 2 Schematic of process steps for the fabrication of high-resolution color phosphor screens.

isopropanol as the solvent [29]. PBMA does not form a homogeneous gel at concentrations less than 30 wt% [29]. At lower concentrations and temperatures below 15°C the mixture separates into two phases. However, at the higher concentrations of polymer, the viscosity is very high, which inhibits the movement of phosphors in the electric field. The viscosity for various mixtures of PBMA in isopropanol and 4 g/L phosphors decreased significantly at higher temperatures. Therefore, a gel system must be optimized to gel at an appropriate temperature, yet not be too viscous as to impede EPD of phosphors.

A deposit density of ~1–2 mg/cm^2 of phosphor is required to ensure adequate optical performance [1, 2]. EPD in homogenous solutions of various concentrations of PBMA (10, 20, 30, and 45 wt%) with and without added water (3 vol%) and at various temperatures from 22–60°C was performed. The addition of water did not have a large effect on the viscosity. The addition of Zn_2SiO_4:Mn (P-1) phosphor did not significantly alter the gelation or the viscosity. For the 20 wt% PBMA mixture, water appeared to be a necessary ingredient to have an acceptable phosphor loading. Without the addition of water, the loading was less than 0.50 mg/cm^2. This increased to >1.0 mg/cm^2 for the first deposit with the addition of 3 vol% water. However, the addition of water caused the polymer to precipitate into a sheet-like solid. For the higher concentrations of PBMA the phosphor loading was low. However, successive depositions (using a new cathode) from the same bath resulted in a reduction of phosphor loading after the first deposition. The decrease in deposit weight was determined to be caused by an increase in the local pH at the cathode.

Although EPD of phosphor in a thermoreversible gel has been demonstrated, it does not appear likely that this PBMA system will allow for adequate phosphor deposition due to the high viscosity at the required

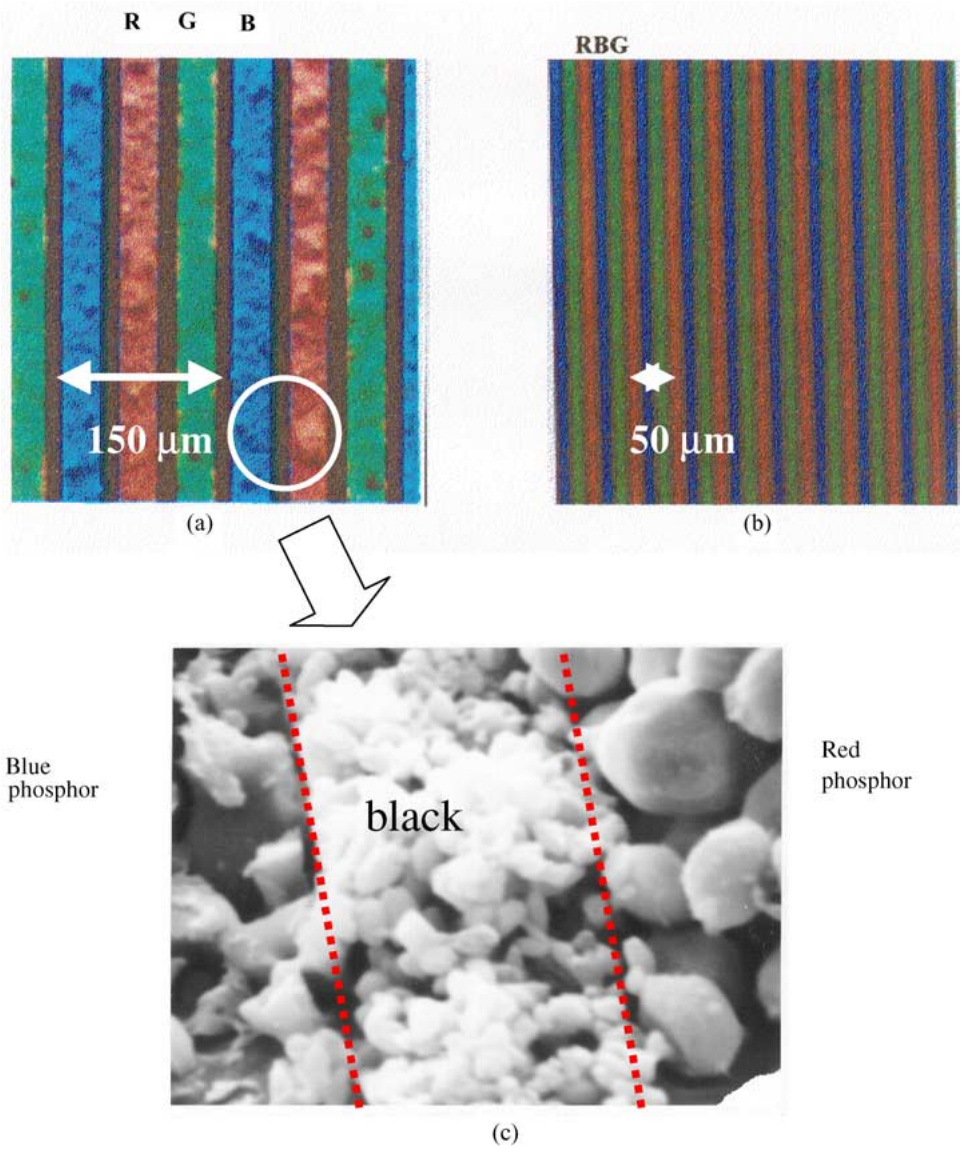

Figure 3 Photomicrographs taken under UV illumination of three-color phosphor screens (a) with triad pitch of 150 μm fabricated on a silicon substrate and (b) with triad pitch of 50 μm on a quartz substrate; (c) SEM micrograph showing filling of black $MnCO_3$ material in between two phosphor lines.

concentration of PBMA for gelation. Therefore, either a lower molecular weight PBMA [30] or a new polymer-solvent system [31] with better gelation characteristics needs to be found for this proposed deposition method of phosphor.

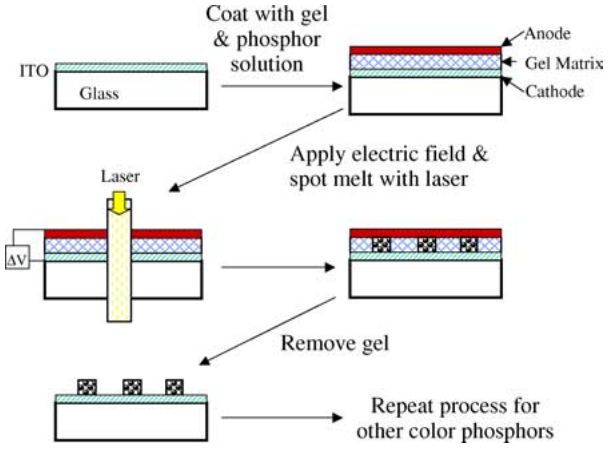

Figure 4 Schematic of the process for EPD in a thermoreversible gel.

6. Conclusions

New flat panel display technologies, such as field emission displays and plasma displays, are placing more stringent requirements on the phosphor screen. Practices of lacquering and then aluminizing the phosphor deposit are often inappropriate for the newer, advanced displays. Electrophoretic deposition of phosphor particles is well suited to deposit the fine (<1 to 10 μm diameter) particles needed for high resolution displays. Although the processing requirements in this study were directed towards the potential use of the screen for FEDs, the process is a general phosphor screening procedure applicable to other applications. In fact, EPD has been used for the manufacturing of CRT [4] and plasma displays [31]. Additionally, EPD can be used as a method to make samples to test new phosphor, as the process does not alter the inherent optimal performance of the phosphor [32].

In order to electrophoretically deposit a wide variety of phosphors (and other powders), the fundamentals of the EPD process were studied. By investigation of the dissociation behavior of nitrate salts in IPA,

measurement of the effects of pH and nitrate salt concentration on the zeta potential of the particles, and by studying the EPD process conditions and modeling the deposition rates, the fundamentals of the EPD have been well-characterized. The electrochemical precipitation reactions which form the adhesive agents were identified and even utilized (without phosphor) to form hydroxide precursors for superconducting films [33]. These fundamental studies not only allow better design of the process for the EPD of phosphors, but for other powdered materials (e.g. zeolites [34]).

As discussed, a major limitation of EPD phosphor deposits has been the low adhesion strength of the deposit. Our research has provided a better understanding of the adhesion of EPD phosphor particles and techniques to enhance the adhesion strength to meet the requirements of these new display technologies. The single greatest effect on the adhesion strength was the added 2 vol% glycerin to the deposition bath.

The ability to improve the adhesion strength of an EPD phosphor deposit is useless if the optical performance is degraded. The color and brightness of screens made with these deposition conditions were unchanged by the processing conditions. EPD phosphor screens also only outgas H_2, CO, CO_2 and low level hydrocarbons under electron bombardment in FED tests [35], which make them attractive for use. Recently, it has been pointed out that the choice of anode is important in EPD of phosphors as corrosion products can degrade the optical performance of the deposited phosphor [36].

New methods to fabricate full-color screens were proposed. Application of photolithography to electrophoretically deposited phosphor films has been successfully demonstrated for the fabrication of high resolution color phosphor screens. Methods combining EPD and standard photolithography have a great potential in patterning novel materials having micro/nano scale particles. The EPD in a thermoreversible gel was explored but needs further work to find a polymer-solvent system with better gelation characteristics than the PBMA polymer used.

Acknowledgements

The authors acknowledge all of the students, postdoctoral researchers and industrial colleagues who contributed to the many years of research on the EPD of phosphors. The research was supported by Hughes Aircraft Co., Electroplasma Inc., Candescent Technology Corp., the UC MICRO Program, the American Display Consortium, the DARPA Phosphor Technology Center of Excellence, Sony Electronics, Inc., and the UC SMART Program. The facilities of SRI International, Menlo Park and Coloray, Fremont, CA were used for the photolithography work. The trilayer process was developed with the help of L. Ternullo and F. Seiferth at the integrated circuit fabrication facility of Microelectronic Engineering Department of RIT. The luminescent workstation funded by the NSF DMR 9626371 equipment grant was used in this study.

References

1. L. OZAWA, "Cathodoluminescence" (Kodansha Ltd., Tokyo, 1990).
2. K. Y. SASAKI and J. B. TALBOT, *Adv. Mater.* **11**(2) (1999) 91.
3. P. F. GROSSO, R. E. RUTHERFORD, JR. and D. E. SARGENT, *J. Electrochem. Soc.* **117** (1970) 1456.
4. E. SLUZKY and K. HESSE, *ibiid.* **136** (1989) 2724.
5. M. J. SHANE, J. B. TALBOT, R. D. SCHREIBER, C. L. ROSS, E. SLUZKY and K. R. HESS, *J. Coll. Interf. Sci.* **165** (1994) 325.
6. B. E. RUSS and J. B. TALBOT, *J. Electrochem. Soc.* **145**(4) (1998) 1245.
7. M. J. SHANE, J. B. TALBOT, E. SLUZKY and K. R. HESSE, *Coll. Surf.* **96** (1994) 301.
8. J. A. SIRACUSE, J. B. TALBOT, E. SLUZKY and K. R. HESSE, *J. Electrochem. Soc.* **137** (1990) 346.
9. J. A. SIRACUSE, J. B. TALBOT, E. SLUZKY, T. AVALOS and K. R. HESSE, *ibid.* **137** (1990) 2336.
10. M. J. SHANE, J. B. TALBOT, B. G. KINNEY, E. SLUZKY and K. R. HESS, *J. Coll. Interf. Sci.* **165** (1994) 334.
11. B. E. RUSS, J. B. TALBOT and E. SLUZKY, *J. Soc. Inform. Displ.* **4**(3) (1996) 207.
12. B. E. RUSS and J. B. TALBOT, *J. Electrochem. Soc.* **145**(4) (1998) 1245.
13. S. LUO and J. B. TALBOT, *ibid.* **148**(7) (2001) H73.
14. S. K. KURINEC and E. SLUZKY, *J. Soc. Inform. Displ.* **4**(4) (1996) 371.
15. D. C. CHANG, J. B. TALBOT, R. P. RAO and C. HOLLAND, *J. Soc. Inform. Displ.* **8**(1) (2000) 51.
16. Y. CHOI and J. B. TALBOT, *ibid.* **10**(3) (2002) 259.
17. B. E. RUSS and J. B. TALBOT, *J. Adhesion* **68** (1998) 257.
18. J. MIZUGUCHI, K. SUMI and T. MUCHI, *J. Electrochem. Soc.* **130** (1983) 1819.
19. S. CERULLI, U.S. Patent no. 2,851,408 (1970).
20. J. A. GUPTON, U.S. Patent no. 3,681,223 (1970).
21. D. M. PHILIPS, U.S. Patent no. 3,904,502 (1973).
22. S. KAPLAN, C. LIBMAN and D. WAINSCOTT, U.S. Patent no. 4,130,472 (1978).
23. J. B. MAHONEY, U.S. Patent, no. 4,990, 416, (1991).
24. E. SLUZKY, S. KURINEC, K. HESSE and L. TERNULLO, US Patent no. 5,582,703 (1996).
25. E. SLUZKY, private communication (2002).
26. S. H. KWON, S. H. CHO, J. S. YOO and J. D. LEE, *J. Electrochem. Soc.* **147**(8) (2000) 3120.
27. J. GUENET, "Thermoreversible Gelation of Polymers and Biopolymers" (Academic Press, San Diego, 1992).
28. R. W. POWERS, *J. Electrochem. Soc.***122** (1975) 490.
29. T. SCHNEIDER, B. A. WOLF, H. KASTEN and F. KREMER, *Macromolecules* **24** (1991) 5387.
30. L. M. JELICH, S. P. NUNES, E. PAUL and B. A. WOLF, *ibid.* **20** (1987) 1943.
31. B. S. JEON, K. Y. HONG, J. S. YOO and K. WHANG, *J. Electrochem. Soc.* **147**(11) (2000) 4356.
32. L. E. SHEA *Interface* **7**(20) (1998) 24.
33. S. B. ABOLMAALI and J. B. TALBOT, *J. Electrochem. Soc.* **140**(2) (1993) 450.
34. C. B. AHLERS and J. B. TALBOT, *ibid.* **146**(9) (1999) 3259.
35. M. E. MALINOWSKI, K. D. STEWART, D. A. A. OHLBERG, T. E. FELTER, A. G. CHAKHOVSKOI, C. HUNT, L. SHEA, B. E. RUSS, J. B. TALBOT and J. MCKITTRICK, in Proceedings of 8th Intern. Conf. on Vacuum Microelectronics, IVMC-95 (Electron Device Society and IEEE, Portland, Oregon, 1995) p. 202.
36. C. GIBBONS, X. P. JING, J. SILVER, A. VECHT and R. WITHNALL, *Electrochem. Solid State Lett.* **2**(7) (1999) 357.

Received 6 January
and accepted 31 January 2003